PAPER

Check for updates

Catalyst-free dynamic transesterification towards a high-performance and fire-safe epoxy vitrimer and its carbon fiber composite†

Jia-Hui Chen, Bo-Wen Liu, Jia-Hui Lu, Peng Lu, Ya-Ling Tang, Li Chen [iD] * and Yu-Zhong Wang

The preparation of fire-safe and high-performance carbon fiber reinforced composites with reprocessable resin matrix and recyclable reinforced fibers is of great importance and particularly urgent to solve the current overreliance on petrochemical resources for composite raw materials. Herein, we propose an effective strategy to simultaneously solve the flammability and nonrecyclability of the epoxy resin-based composites, in the form of fire-safe and catalyst-free dynamic transesterification networks by introducing a phosphaphenanthrene-derived diol as a multifunctional modifier for transesterification without using any toxic catalysts. In this strategy, the phosphaphenanthrene moieties enhanced the fire safety; while the hydroxy groups promoted the construction of catalyst-free dynamic transesterification networks. To our delight, the generated epoxy resin and its composite exhibit excellent mechanical properties, high thermal stability, fire safety, fast repairability and malleability. Furthermore, the resin matrix can be dissolved as the low-mass diol molecules participate in bond exchange reactions to achieve CFs with nearly 100% recyclability.

Introduction

Carbon fiber-reinforced epoxy resin composites (EP/CFs) with high strength-to-weight ratios, excellent durability and corrosion resistance have seen explosive growth in various applications, especially in some high-tech fields with fire-safe demands.[1] Fire-safe EP/CFs are usually established through integrating flame retardants/flame-retardant groups into epoxy resins (EPs). With an increase in the amounts of fire-safe EP/CFs being used,[2] their waste materials, including off-cuts during manufacturing and end-of-life materials, are reaching a significant level, which causes environmental concern for fire-safe EP/CF waste. In addition, these fire-safe materials also bring about the new problem of recycling or disposal.[3] Due to the cross-linked structure of EPs, most fire-safe EPs and EP/CFs and their waste have been disposed of by incineration, releasing toxic or harmful gases into the atmospheric environment and causing serious atmospheric pollution.[4] Therefore, the flame retardants in these materials usually need to be

removed once recycled, resulting in greatly increased disposal costs. Consequently, how to solve the recycling or disposal of fire-safe EPs and their composites still presents urgent challenges.

We envision that the fire-safety and recyclability of EP/CFs could be achieved by combining flame-retardant groups and dynamic covalent bonds in the crosslinked networks (covalent adaptable networks, CANs) of EPs. Different CANs, including dissociative and associative ones, have been demonstrated as a route to combine processability, reparability, and high performance once being crosslinked.[5] Among these dynamic covalent reactions,[6] transesterification has been widely reported because the exchange reaction mechanism is conveniently applied to the commercially available epoxy-acid/anhydride curing systems.[7] However, most of these epoxy vitrimers depend on transesterification catalysts[8] with high cost, toxicity and low solubility in organic compounds.[9] By adding suitable active low-mass diols/polyols, these abundant primary hydroxyls show much higher reactivity than the β-hydroxyls of the conventional epoxy-acid/anhydride curing systems where the transesterification catalysts are necessary. Consequently, such diols/polyols can activate the dynamic transesterification and promote the topology rearrangement of the cured networks in the absence of transesterification catalysts.[10]

A potential and effective method for simultaneously addressing the nonrecyclability and flammability of EPs is to design fire-safe epoxy vitrimers. As a typical hetero-ester bond, phosphate with a representative flame-retardant element (phos-

The Collaborative Innovation Center for Eco-Friendly and Fire-Safety Polymeric Materials (MoE), National Engineering Laboratory of Eco-Friendly Polymeric Materials (Sichuan), State Key Laboratory of Polymer Materials Engineering, College of Chemistry, Sichuan University, Chengdu 610064, China.
E-mail: l.chen.scu@gmail.com
†Electronic supplementary information (ESI) available. See DOI: https://doi.org/10.1039/d2gc01405j

phorus) can also undergo a thermal rearrangement reaction *via* transesterification to endow the thermosets with fire-safety and reprocessability.[11] However, compared with the C–O bond in carboxylates, the bond energy of P–O is far below, resulting in bond rupture easily generating phosphoric acid and polyhydroxy compounds upon heating, and dramatically worsening the thermal stability of the resulting thermosets ($T_{5\%} <$ 250 °C).[12] Different from phosphate, phosphaphenanthrene and its derivatives with high efficacy, low toxicity, and acceptable economic efficiency[13] can easily be chemically introduced into the cured thermosets, and endow the resulting materials with long-lasting fire safety and excellent thermal stability.[14] Given all that, we propose a new sustainable and fire-safe strategy based on the above-mentioned catalyst-free dynamic transesterification. The direct construction of fire-safe epoxy vitrimers with catalyst-free dynamic transesterification effectively solves the problem of the recycling or disposal of fire-safe EPs and their composites.

Herein, we employed the commercially available phosphaphenanthrene-based diol named 6-(2,5-bis(2-hydroxyethoxy) phenyl)dibenzo[*c*,*e*] [1,2]oxaphosphinine 6-oxide (DHH) as a typical representative to demonstrate the proposed strategy, and to further explore the relationship between the fire safety and dynamic transesterification of the vitrimers. DHH was used as a multifunctional transesterification modifier to estab-

lish the fire-safe and catalyst-free epoxy vitrimer (Fig. 1c), and as a way to "kill two birds with one stone", appropriate recycling performance and satisfactory fire safety were exhibited by the resultant EP vitrimer simultaneously. Both the vitrimer and its composite possessed high mechanical properties, high thermal stability ($T_{5\%} >$ 380 °C), fire-safety efficacy and reprocessability. More importantly, owing to the dynamic ester-linkages, the epoxy vitrimer could be dissolved in ethylene glycol (EG) as the dihydroxy molecules participated in bond exchange reactions to achieve CFs with nearly 100% recyclability. Taking advantage of these features, we offer a sustainable and fire-safe strategy for designing intrinsically flame-retardant carbon fiber reinforced composites composed of reprocessable resins and recyclable fibers.

Results and discussion

This new material is an advance on the contradictory performance observed between fire-safety and reprocessability, as well as the low mechanical properties of traditional fire-safe materials. DGEBA, AA and DHH (or HQEE) were formulated in different molar ratios and they readily formed AAD-EP through a one-step reaction (Fig. S1 and Table S1†). First, the effect of different amounts of DHH on the curing behaviors of AAD-EP
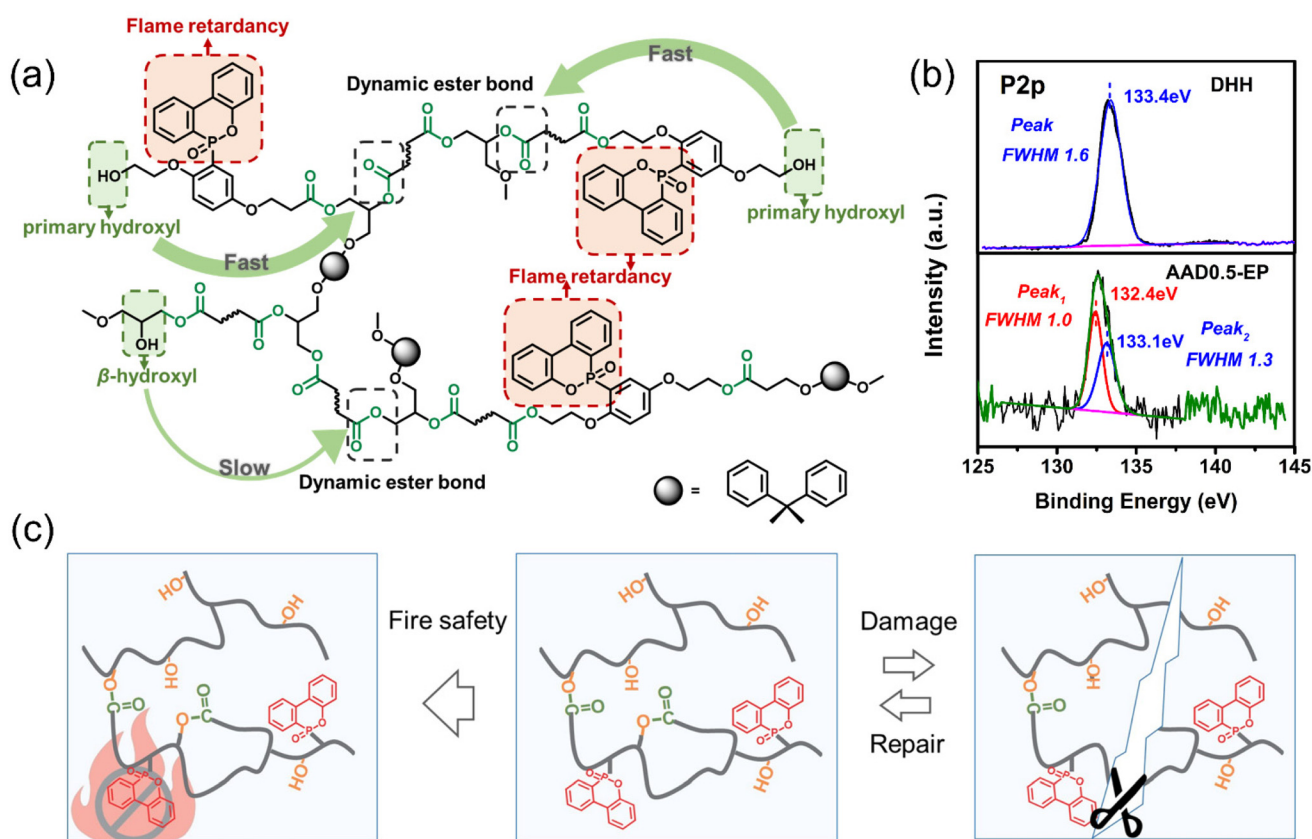

Fig. 1 (a) Illustration of the chemical structures in the presence of DHH; (b) XPS P 2p spectra of DHH and AAD0.5-EP; (c) proposed mechanisms of how DHH contributes to the repair, recycling and fire safety of epoxy vitrimers.

was investigated by DSC thermograms (Fig. S2†). Obviously, as the DHH loading increased to AAD0.5-EP, the curing exothermic peak temperature decreased from 216.6 °C to 206.8 °C, indicating that DHH could promote the curing reaction activity between the acid and epoxy. In addition, the non-isothermal curing behaviors with different heating rates from 5 to 20 °C min⁻¹ further demonstrated that DHH was effective in reducing the activation energy of the AAD-EP (Fig. S3†). The abundant primary hydroxyls in DHH appeared weakly acidic, were beneficial for increasing the content of active hydrogen in AAD-EP, promoted the ring-opening reaction between the –COOH group and epoxy, and further accelerated the reactivity of the curing reaction.

To better illustrate the detailed curing routes of AAD-EP, X-ray photoelectron spectroscopy (XPS) was performed to obtain the P 2p high-resolution spectra of AAD0.5-EP and DHH (Fig. 1b). Clearly, the P 2p spectrum of DHH displayed a peak at 133.4 eV, while the P 2p signal of AAD0.5-EP was divided into two peaks at 132.4 eV and 133.1 eV. In general, the variation in P 2p binding energy is related to the change in the relevant P environment.[15] The chemical environment of DHH changed, which was attributed to the transesterification between the ester linkage and the primary hydroxyls of DHH. One case was that one of the hydroxyls in DHH was chemically bonded with EP, and the other case was that both the primary hydroxyls in DHH were completely incorporated into EP, resulting in the appearance of two P 2p signal peaks. Accordingly, the chemical structures of AAD-EP in the presence of DHH were proposed, as shown in Fig. 1a. According to the FT-IR (Fig. S4†), the chemical structures of AAD-EP were

characterized. In the FTIR spectrum of AA, the absorptions at 1732 cm⁻¹ and 3440 cm⁻¹ corresponded to the stretching vibrations of C=O and O−H in the –COOH group, respectively. For AA-EP and AAD0.5-EP, the absorptions for C=O shifted to higher wavenumbers due to the formation of ester bonds by reaction between the epoxy and –COOH groups. Moreover, in the FTIR spectra of AA-EP and AAD0.5-EP, newly emerging peaks at approximately 3430 cm⁻¹ appeared, belonging to the stretching vibrations of the β-hydroxyl and abundant primary hydroxyls. In addition, the absorption for the epoxy group at 915 cm⁻¹ in the spectra of AA-EP and AAD0.5-EP almost disappeared, indicating the complete reaction of epoxy groups. Meanwhile, combined FT-IR spectral analysis and the results of the gel fraction and swelling ratio (Fig. S5†) proved AAD-EP with a complete cross-linked network.

To evaluate the thermomechanical behaviors of AAD-EP, dynamic mechanical analysis (DMA) was performed on AAD-EP (Fig. 2 and Table S2†). For each composition, there was only a one-step change in E' and a single peak in $\tan \delta$. When the loading of DHH increased, E' at 25 °C increased from 2906 MPa for AA-EP to 3179 MPa for AAD0.5-EP, mainly due to the enhanced rigid backbone of EP. Then, the cross-linking densities (ν_e) of AAD-EP were calculated using the rubber elasticity equation:[1b]

$$\nu_e = E_r/3RT,$$

where E_r is the storage modulus at temperature T (T_α + 30 K), and R is the universal gas constant (8.314 J mol⁻¹ K⁻¹). The calculated results (Table S2†) revealed that the incorporation of DHH into AA-EP could reduce the cross-linking density of
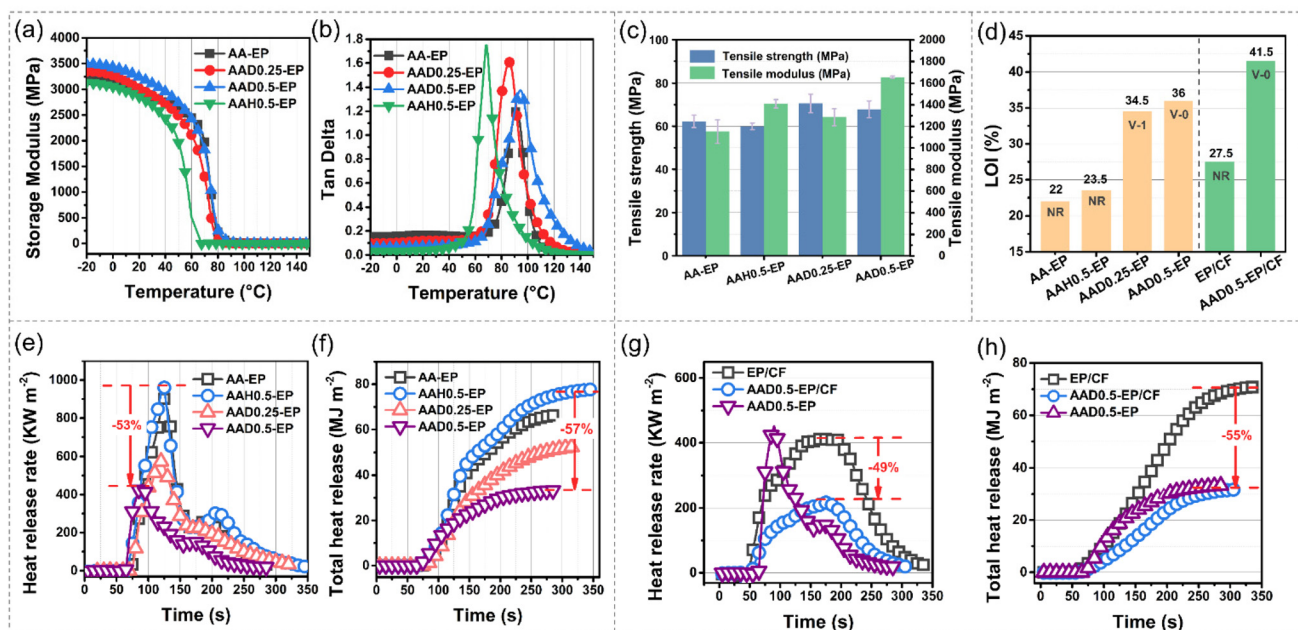

Fig. 2 (a) The DMA curves of storage modulus and (b) tan δ versus temperature for AAD-EP and the control sample AAH0.5-EP; (c) tensile strength and modulus; (d) the LOI and UL-94 rating; (e) the HRR plots and (f) THR plots of AAD-EP and AAH0.5-EP, (g) the HRR plots and (h) THR plots of EP/CF, AAD0.5-EP/CF and AAD0.5-EP obtained from cone calorimetry.

the epoxy network and enhance the rigidity of the backbone. The T_α value is dependent on both the network stiffness and cross-linking density,[16] thus, AAD0.5-EP exhibited the highest T_α value (Table S2†). For AAD0.25-EP, the value of T_α was lower than that of AA-EP, because the cross-linking density decreased. The control sample AAH0.5-EP having the lowest T_α, was attributed to both the flexible backbone and not high crosslink density. Clearly, the glass transition temperature (T_g) of AAD-EP was measured *via* DSC, which showed a similar trend to the T_α value (Table S2†).

All samples exhibited typical brittle rupture (Fig. 2c), and AAD0.25-EP had the highest tensile strength (σ) of 70.5 MPa. As the content of DHH increased to AAD0.5-EP, the value of σ appeared slightly decreased to 67.8 MPa. The phenomenon was caused by a combination of the cross-linking density and phosphaphenanthrene rigid structure. When the DHH content was low, the phosphaphenanthrene rigid structure played a major role, and when the DHH content was increased to AAD0.5-EP, the reduced cross-link density became dominant; thus, the σ of AAD-EP first increased and then decreased. Interestingly, the σ values of AA-EP and AAH0.5-EP were 62.2 MPa and 60.0 MPa, respectively, both lower than that of AAD0.5-EP, which suggested that the reduced cross-link density of AAD0.5-EP did not sacrifice the mechanical properties of EP. In addition, Young's modulus (E) gradually increased as the DHH content increased; when the DHH content increased to AAD0.5-EP, the E value reached a maximum value of 1657 MPa.

In EPs, phosphaphenanthrene and its derivatives with high initial degradation temperatures play a positive role in the thermal properties of the resulting materials.[14] The thermal stability of AAD-EP was characterized by TGA under N_2 and air atmospheres (Fig. S6† and Table 1). Under a N_2 atmosphere, the initial decomposition temperatures (a temperature with 5% mass loss, $T_{5\%}$) of AAD0.25-EP and AAD0.5-EP were 385.3 °C and 385.1 °C, respectively, which were close to the value of AA-EP (392 °C). Under an air atmosphere, all the AAD-EPs unsurprisingly exhibited excellent thermal stability, and the $T_{5\%}$ values were even superior to that of AA-EP. Although the maximum decomposition temperature (T_{max}) of AAD-EP was slightly decreased in N_2 and air atmospheres, the $T_{max,2}$ of AAD-EP was much higher than that of AA-EP. Furthermore, it was found that, either in the N_2 or air atmosphere, the T_{max} of AAH0.5-EP was close to the value of AAD0.5-EP, indicating that T_{max} slightly decreased owing to the reduced cross-link density, not the premature decomposition

of DHH. A possible reason was that the incorporation of DHH stabilized the char, delayed the oxidation of AAD-EP at higher temperatures and increased the $T_{max,2}$ value of AAD-EP, which was distinctly different from ordinary phosphorus-containing flame retardants.[17] In brief, AAD-EP exhibited excellent thermal stability, and the values of $T_{5\%}$ and T_{max} were close to those of commercial EP.[18]

The limiting oxygen index (LOI) and a UL-94 vertical burning test were used to evaluate the fire safety of AAD-EP. The results (Fig. 2d and Table S3†) showed that the LOI values of AA-EP and AAH0.5-EP were 22% and 23.5%, respectively, and both failed to pass UL-94 ratings, indicating high flammability. In contrast, the desired fire-safety was displayed in AAD-EP when DHH was incorporated into the EP structure. As the loading of DHH increased to AAD0.25-EP and AAD0.5-EP, the LOI values obviously improved to 34.5% and 36.0%, respectively. Moreover, AAD0.5-EP easily achieved a UL-94 V-0 rating and exhibited high fire safety; thus AAD0.5-EP as prepregs was used to prepare a carbon fiber-reinforced composite, namely AAD0.5-EP/CF, according to the procedure described in the Experimental section. The LOI value of AAD0.5-EP/CF was 41.5% and passed the UL-94 V-0 rating, while the LOI value of EP/CF was only 27.5% and hardly passed the UL-94 rating (Fig. 2d). The application of highly fire-safe AAD0.5-EP was effective in improving the fire-safety of its carbon fiber composite.

Different from small bench-scale tests like LOI and UL-94, cone calorimetry provides a burning scenario similar to that of a real fire,[19] to further evaluate the burning behaviors of AAD-EP (Fig. 2 and Table S3†). The peak heat release rate (PHRR) and total heat release (THR) of AAD-EP, as two important parameters to evaluate fire safety, decreased gradually with an increase of the DHH content. In particular, AAD0.5-EP exhibited the lowest PHRR and THR values of 451.8 kW m^{-2} and 33.2 MJ m^{-2}, respectively, which were 53% and 57% lower than those of AAH0.5-EP. Both the average effective heat combustion (Av-EHC) and the maximum average heat rate emission (MAHRE) of AAD-EP also exhibited remarkable reduction with increasing DHH content, indicating that DHH effectively slowed flame propagation. Furthermore, the char residue of AAD0.5-EP of 12.4% was more than the value of AA-EP (3.2%) and AAH0.5-EP (3.9%) after burning. The reason was that the phosphaphenanthrene moieties in DHH were oxidized to phosphorus pentoxide (P_2O_5) and then hydrolyzed to poly/ultra/pyrophosphoric acid(s) (HxPyOz) during the combustion process, which was beneficial for promoting the charring

Table 1 Thermal analysis data of AAD-EP and AAH0.5-EP

Sample	N_2			Air			
	$T_{5\%}$ (°C)	T_{max} (°C)	W_{700} (%)	$T_{5\%}$ (°C)	$T_{max,1}$ (°C)	$T_{max,2}$ (°C)	W_{700} (%)
AA-EP	392.0	445.7	14.1	359.0	439.3	584.6	0.1
AAD0.25-EP	385.3	431.6	16.5	371.6	433.6	611.6	3.4
AAD0.5-EP	385.1	435.5	16.4	362.0	425.4	619.8	10.8
AAH0.5-EP	369.2	434.6	9.0	368.4	430.2	565.3	1.8

process and generating higher residues.[20] Then, the cone calorimetry experiment was further used to assess the burning behaviors of AAD0.5-EP/CF (Fig. 2 and Table S4†). Compared with EP/CF, the reduction in the PHRR and THR values of AAD0.5-EP/CF was up to 49% and 55%, respectively, demonstrating that AAD0.5-EP/CF has excellent fire safety. To explore the fire-safety protection mechanism of DHH in the AAD-EP system, SEM (Fig. S7a₁–a₄†), Raman spectroscopy (Fig. S7b₁– b₄†) and TG-FTIR (Fig. S8†) tests were conducted. Combining SEM micrographs, Raman spectroscopy and TG-FTIR tests illustrated that DHH had positive flame-retardant activity in both the condensed and gas phases.

To research the catalyst-free transesterification mechanism, the transesterification between primary hydroxyls and ester linkages was discussed *via* the model molecule experiment, and the chemical change was monitored by ^{1}H NMR. Model compound 1 (1 eq.) (Fig. S9†) and ethylene glycol (EG) (1 eq.) were mixed into a glass flask and heated at 150 °C under a gentle nitrogen flow, aiming to undergo the transesterification process and generate the exchange products (Fig. 3a). Then, aliquots were taken from the mixture at different times and dissolved in DMSO-d_6, and the chemical change was monitored by ^{1}H NMR (Fig. 3b).

Obviously, as exchange reaction occurred, the signal corresponding to -C_2H_4 in EG structures gradually disappeared in the real-time ^{1}H NMR spectrum and was replaced by the signal corresponding to –C_2H_4 in the formed new ester linkages, indicating that primary hydroxyls of EG increasingly participated in transesterification. At 20 h, the signal corresponding to –C_2H_4 in EG structures fully disappeared, and the ^{1}H NMR spectrum no longer changed. This phenomenon proved that the primary hydroxyls in AAD-EP spontaneously attacked the ester bond at a certain temperature, and activated dynamic transesterification, resulting in the topology rearrangement and showing the malleability of EP.

The dynamic network undergoes a secondary bond exchange reaction at elevated temperatures, resulting in an epoxy network with certain thermoplastic behavior, such as malleability, reparability and reprocessability.[6] To assess the malleability of AAD-EP, stress relaxation experiments were conducted. According to the Maxwell model, the relaxation time (τ^*) is defined as the time needed to relax to 63% of the initial modulus.[21] As shown in the stress relaxation curves of AAD-EP and AAH0.5-EP (Fig. 3c), AA-EP had a fairly long τ^* value of more than ~10 000 s. As the DHH content increased, the τ^* value of AAD-EP decreased, along with a clear acceleration of the relaxation rate. Compared with AAH0.5-EP, the τ^* value of AAD0.5-EP was lower and exhibited more significant relaxation behavior, indicating that the phosphaphenanthrene moieties in DHH did not affect the topology rearrangement of the dynamic network. The AAD0.5-EP exhibited a lower τ^* value than AAD-EP, which revealed that the primary hydroxyls of DHH could tune the rate of stress relaxation and promote dynamic transesterification. Interestingly, high temperatures were also beneficial for promoting dynamic transesterification (Fig. 3d). At 180 °C, the τ^* value of AAD0.5-EP was more than ~10 000 s; when the relaxation temperature increased to 200 °C and 220 °C, the τ^* value decreased with it. Clearly, as the relaxation temperature increased, the rate of stress relaxation accelerated, and the τ^* value of AAD-EP decreased.

To investigate the mechanical properties after reprocessing, AAD0.5-EP as a typical example, was selected to discuss the relationship between the reprocessing time and recycled tensile strength (Fig. 4a). Firstly, the recycling efficiency is defined as the ratio of the tensile strength of the reprocessed sample to that of the original sample.[22] The AAD0.5-EP was reprocessed into specimens with a standard dumbbell shape for tensile testing through compression molding at 220 °C under 10 MPa for different times. As the reprocessing time of AAD0.5-EP increased, recycled tensile strength increased, and
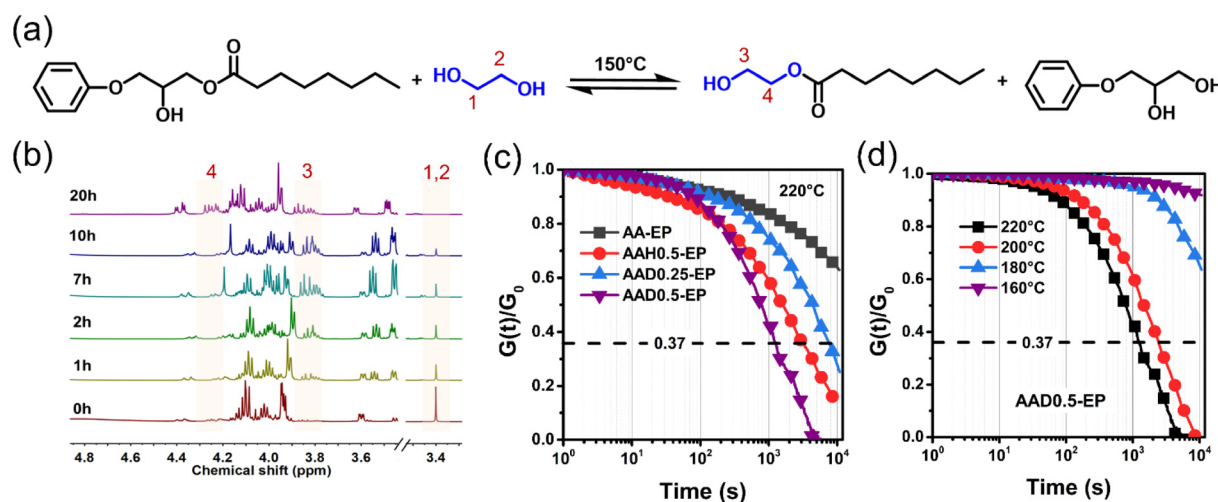

Fig. 3 (a) The transesterification process between free –OH groups and ester linkages and the exchange products; (b) the real-time ^{1}H NMR spectra of the mixture after adding EG for different times at 150 °C; (c) the stress relaxation curves of AAD-EP and AAH0.5-EP; (d) the stress relaxation curves of AAD0.5-EP at different temperatures.
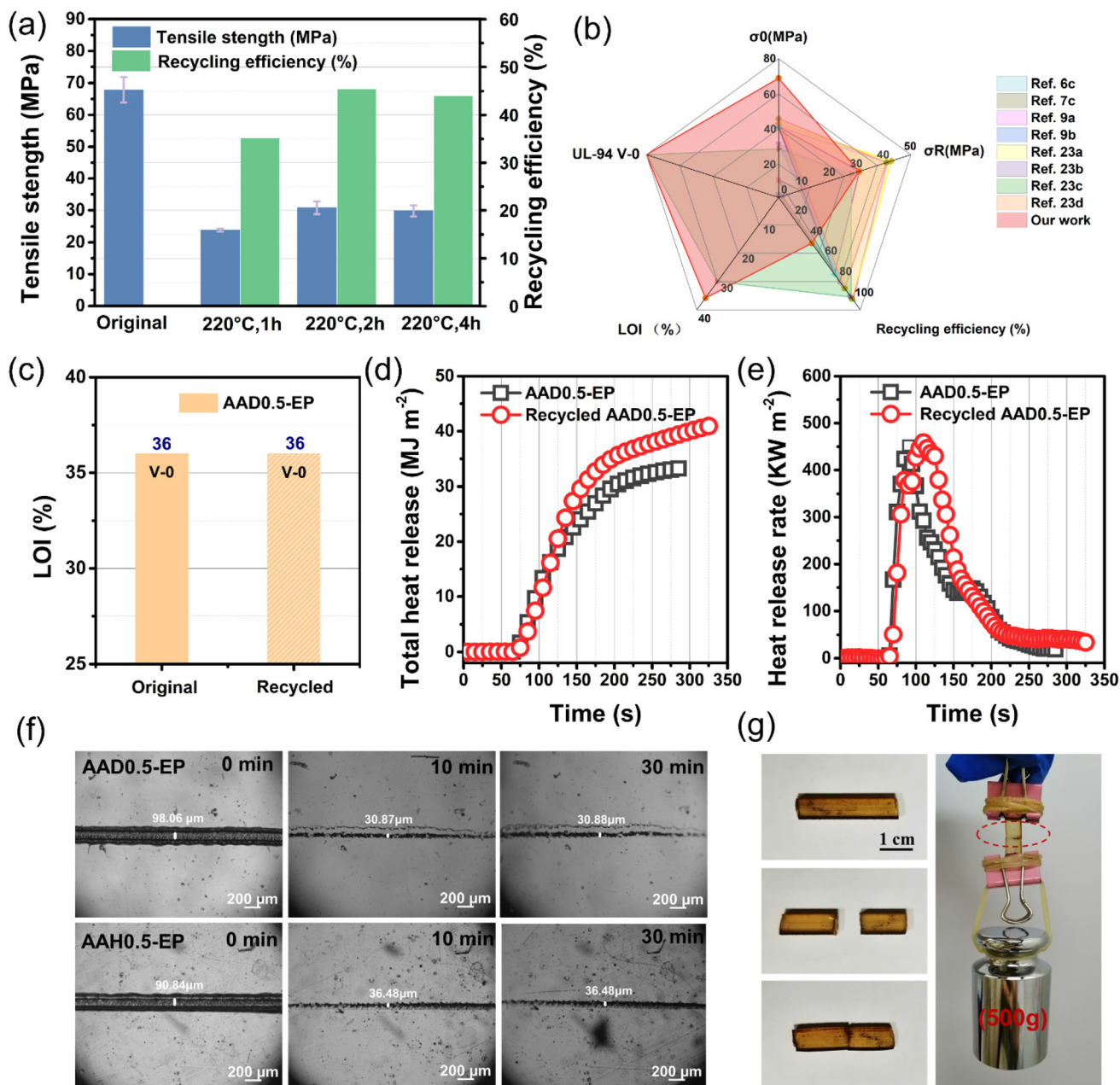
Fig. 4 (a) The tensile strength and recycling efficiency of AAD0.5-EP at different reprocessing times; (b) the original and recycled tensile strength, recycling efficiency and fire-safety parameters of AAD0.5-EP compared with published epoxy vitrimers; (c) the LOI and UL-94 rating; (d) the HRR and (e) the THR plots of the original and recycled AAD0.5-EP obtained from cone calorimetry; (f) the images of AAD0.5-EP and AAH0.5-EP at 200 °C with different repair times; (g) illustration of the welding property of AAD0.5-EP.

the recycling efficiency increased; when the reprocessing time was 2 h, the recycling efficiency reached a maximum value of ~44.6%, and it no longer increased. Although the recycling efficiency was also affected by different reprocessed pressure, the recycling efficiency was not improved with a further increased pressure of compression molding (Fig. S10†). Then, the tensile fracture surfaces of the reprocessed AAD0.5-EP at different reprocessing times were observed through SEM images (Fig. S11†) to explore the factors affecting the recycling efficiency of AAD0.5-EP. It was found that the original AAD0.5-EP had a smooth fracture surface, while the reprocessed sample was rough. The result indicated that the dynamic transesterification in AAD0.5-EP only appeared in the close contact area between neighboring particles and did not occur in the entire cross-linked epoxy network, leading to the incomplete recovery of the tensile strength. In addition, the absence of transesterification catalysts[10] within AAD0.5-EP also made the product harder with high recycling efficiency. Then, the mechanical properties, recycling efficiency and fire-safe parameters of AAD0.5-EP were compared with published epoxy

vitrimers (Fig. 4b and Table S5†).[23] The original tensile strength (σ_0) and fire safety of AAD0.5-EP were much higher than those of epoxy vitrimers reported in the literature. Although the recycling efficiency was not high, the recycled tensile strength (σ_R) of AAD0.5-EP was close to or even better than that of most of the published epoxy vitrimers.

The fire safety of AAD0.5-EP after reprocessing was further explored. The unchanged LOI value and UL-94 V-0 rating (Fig. 4c) of the reprocessed AAD0.5-EP manifested that the fire safety of AAD0.5-EP was not deteriorated by reprocessing. In HRR and THR plots (Fig. 4 and Table S6†), compared to the original plots, the HRR and THR plots of the reprocessed AAD0.5-EP were also unchanged, which provided evidence that the fire safety of reprocessed AAD0.5-EP remained after reprocessing. The burning residue of the original and reprocessed AAD0.5-EP obtained from cone calorimetry was investigated through SEM micrographs and merged EDX elemental mapping images (Fig. S12†). The residue of the original and reprocessed AAD0.5-EP both showed smooth and dense char surfaces, and the merged EDX elemental mapping images of the char indicated that phosphorus was evenly distributed in the residues, leading to no loss in the fire safety of AAD0.5-EP after reprocessing.

We were motivated by the evidence that the primary hydroxyls in DHH could accelerate dynamic transesterification to achieve excellent reprocessibility of AAD0.5-EP. Thus, were the primary hydroxyls in DHH beneficial for the repair of AAD0.5-EP in the same way? Fig. 4f shows images of the repairing process of cracks of AAD0.5-EP and AAH0.5-EP for different times. The repair process was conducted by simply sandwiching the film sample between two metal plates and placing them in an oven at 200 °C for different times. Through an optical microscope, the crack of AAD0.5-EP recovered ~69% within 10 min, while the crack of AAH0.5-EP only recovered ~60%, illustrating that the repair of AAD0.5-EP was better than that of AAH0.5-EP under the same conditions, and the phosphaphenanthrene moieties in the DHH structure did not deteriorate the repair property of AAD0.5-EP, which was consistent with the conclusion of the stress relaxation experiment. Based on the rapid repair of AAD0.5-EP, the welding property of AAD0.5-EP was further investigated. Two fragments from AAD0.5-EP were laterally stacked together and sandwiched between two metal plates in an oven at 200 °C for 1 h. Then, the two fragments were firmly welded due to dynamic transesterification, and the newly formed welding sample could hold a weight of ~500 g (Fig. 4g). Meanwhile, the welded AAD0.5-EP was subjected to a tensile test (Fig. S13†), and the tensile strength was ~20.3 MPa, indicating fairly strong bonding at the welded area. These features provide great potential for AAD-EP in versatile applications.

Furthermore, based on dynamic transesterification, the AAD0.5-EP epoxy matrix could be completely degraded in the EG solution, and the nondestructive recycling of CFs was achieved. Fig. 5a shows the recycling process of CF in detail. Obviously, upon increasing the immersion time, the layers of CF appeared separated, and the resin matrix was completely
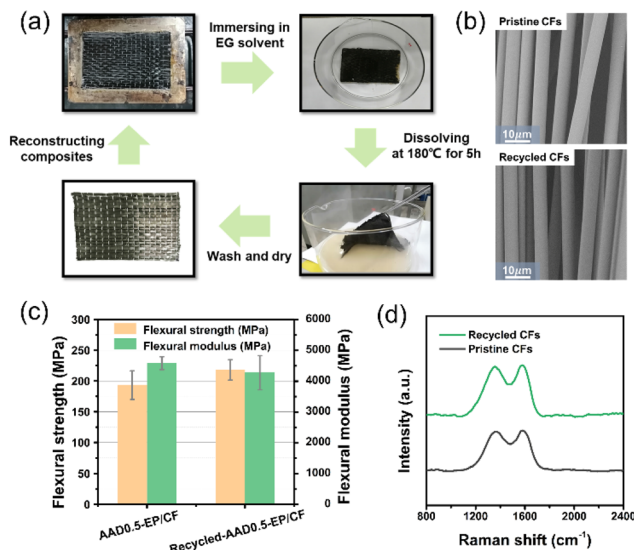

Fig. 5 (a) The nondestructive recycling process of CF in EG solution at 180 °C; (b) SEM of the microscale morphology of the pristine and recycled CFs; (c) the flexural strength and modulus of AAD0.5-EP/CF and recycled AAD0.5-EP/CF; (d) the Raman spectra of pristine and recycled CFs.

dissolved at an immersion time of 5 h, which was due to dynamic transesterification between the primary hydroxyls of EG solution and the ester linkages of AAD0.5-EP at 180 °C. The corresponding alcoholysis products were confirmed by MS analysis (Fig. S14†). Then, the residual solution was washed with ethyl acetate and ethanol and dried at 80 °C for 12 h, and the recycled CFs were obtained. Next, the microscale morphology and chemical structures of recycled CFs were investigated *via* SEM and Raman spectroscopy. SEM proved that the microscale morphology of the recycled CFs was clean and smooth, similar to that of the pristine CFs, and no visible resin residue on the CFs was observed, indicating that the resin matrix was fully removed (Fig. 5b). In the Raman spectra, the signals and peak intensities of recycled CFs were close to those of pristine CFs, which demonstrated that the chemical structure of recycled CFs was not damaged during the recycling process (Fig. 5d). Moreover, the recycled CFs were reused to prepare AAD0.5-EP/CF that was subjected to three-point flexural testing (Fig. 5c). The flexural strength and modulus of recycled AAD0.5-EP/CF did not reduce or even enhance, meaning the recycled CFs still retained excellent mechanical properties. These results manifested that AAD0.5-EP/CF could be degraded under mild conditions, the recycled CFs possessed the same microscale morphology, chemical structures and mechanical properties as the pristine CFs and CFs with nearly 100% recyclability were achieved.

Conclusions

The construction of fire-safe carbon fiber reinforced composites with high performance, composed of reprocessable resin

and recyclable fibers by using intrinsically flame-retardant vitrimers, is an important way to solve the current overreliance on petrochemical resources for composite raw materials. Herein, we advanced a new strategy to effectively solve the problems of flammability and nonrecyclability of EPs and their composites. In our design, the phosphaphenanthrene-based diol DHH was successfully introduced as a multifunctional modifier in an epoxy-acid curing system towards a catalyst-free reprocessable fire-safe epoxy vitrimer and its carbon fiber reinforced composite. Taking advantage of the phosphaphenanthrene moieties in DHH, the phosphorus-containing vitrimer and its composite, denoted as AAD0.5-EP and AAD0.5-EP/CF, respectively, both exhibited high efficiency in anti-ignition performance and reduced the heat released during burning, thus increasing the fire-safety. Chemically, the primary hydroxyls in DHH accelerate dynamic transesterification in the absence of a transesterification catalyst. Due to abundant –OH groups and dynamic ester bonds, AAD0.5-EP possessed versatile reprocessability and rapid repairability (200 °C in 10 min). More importantly, AAD0.5-EP could be degraded in the low-mass diol to achieve CFs with nearly 100% recyclability. The recycled CFs maintained the same level of microscale morphology, chemical structures and mechanical properties as pristine CFs. We foresee an extension of this technology to include other types of thermosets and their composites.

Experimental

Preparation of fire-safety epoxy vitrimers (AAD-EP)

DER332 epoxy resin as a polymer matrix, AA as a curing agent, and DHH as a multifunctional modifier were mixed according to the formulation shown in Table S1.† A homogeneous mixture was obtained by stirring all ingredients for 15 min at 150 °C. Afterward, the viscous liquid mixture was degassed at 130 °C under vacuum for 5 min and then transferred to a Teflon mold immediately. The curing process was performed on a vulcanizing press at 150 °C for 3 h, 180 °C for 2 h, and 220 °C for 3 h to obtain AAD-EP specimens. After curing, the samples were cooled naturally to room temperature before being removed from the mold. For all samples, the molar ratio of –COOH/epoxy was fixed as 1 : 1 as the molar ratio of DHH/epoxy increased from 0 mol to 0.5 mol. The control sample AAH0.5-EP was synthesized according to the same method as AAD0.5-EP, except that DHH was replaced by HQEE, which was used to compare the reprocessability and fire safety of AAD0.5-EP.

Preparation of AAD0.5-EP/CF

The composite was prepared by a hand lay-up technique followed by compression molding. First, seven layers of CF and the mold coated with a thin layer of the release agent were preheated at 130 °C. Then, the precursor AAD0.5-EP was stirred at 150 °C for 15 min, poured on the carbon fabric, placed into a preheated mold and degassed in a vacuum oven at 130 °C for at least 30 min until no bubbles emerged. Finally, the mold was transferred to a vulcanizing press, and the curing process

was the same as the aforementioned curing process of AAD-EP. The obtained composite was named AAD0.5-EP/CF. The fiber mass fraction of AAD0.5-EP/CF is ~67 wt%, and the resulting samples were cut into certain dimensions for the subsequent tests. The EP/CF based on DER332 epoxy resin and AA was prepared via the same method, and the fiber mass fraction was ~60.4 wt%, which was used to compare the mechanical properties and fire safety of AAD0.5-EP/CF.

Conflicts of interest

There are no conflicts to declare.

Notes and references

1 (a) P. Taynton, H. Ni, C. Zhu, K. Yu, S. Loob, Y. Jin, H. J. Qi and W. Zhang, *Adv. Mater.*, 2016, **28**, 2904–2909; (b) Y. Y. Liu, G. L. Liu, Y. D. Li, Y. Weng and J. B. Zeng, *ACS Sustainable Chem. Eng.*, 2021, **9**, 4638–4647; (c) K. Yu, Q. Shi, M. L. Dunn, T. Wang and H. J. Qi, *Adv. Funct. Mater.*, 2016, **26**, 6098–6106; (d) B. Wang, S. Ma, S. Yan and J. Zhu, *Green Chem.*, 2019, **21**, 5781–5796.

2 (a) X. H. Shi, L. Chen, Q. Zhao, J. W. Long, Y. M. Li and Y. Z. Wang, *Compos. Sci. Technol.*, 2020, **187**, 107945; (b) X. Li, J. Zhang, L. Zhang, A. Ruiz de Luzuriaga, A. Rekondo and D. Y. Wang, *Compos. Commun.*, 2021, **25**, 100754; (c) S. Wang, S. Ma, Q. Li, X. Xu, B. Wang, W. Yuan, S. Zhou, S. You and J. Zhu, *Green Chem.*, 2019, **21**, 1484–1497.

3 A. Covaci, S. Harrad, M. A. E. Abdallah, N. Ali, R. J. Law, D. Herzke and C. A. de Wit, *Environ. Int.*, 2011, **37**, 532–556.

4 (a) L. Delva, S. Hubo, L. Cardon and K. Ragaert, *Waste Manage.*, 2018, **82**, 198–206; (b) I. Vollmer, M. J. F. Jenks, M. C. P. Roelands, R. J. White, T. van Harmelen, P. de Wild, G. P. van der Laan, F. Meirer, J. T. F. Keurentjes and B. M. Weckhuysen, *Angew. Chem., Int. Ed.*, 2020, **59**, 15402–15423.

5 (a) Y. Guo, S. Chen, L. Sun, L. Yang, L. Zhang, J. Lou and Z. You, *Adv. Funct. Mater.*, 2021, **31**, 2009799; (b) H. Feng, S. Ma, X. Xu, Q. Li, B. Wang, N. Lu, P. Li, S. Wang, Z. Yu and J. Zhu, *Green Chem.*, 2021, **23**, 9061–9070.

6 (a) C. Ye, V. S. D. Voet, R. Folkersma and K. Loos, *Adv. Mater.*, 2021, **33**, 2008460; (b) N. J. Van Zee and R. Nicolaÿ, *Prog. Polym. Sci.*, 2020, **104**, 101233; (c) Z. Ma, Y. Wang, J. Zhu, J. Yu and Z. Hu, *J. Polym. Sci., Part A: Polym. Chem.*,

2017, **55**, 1790–1799; (*d*) X. M. Ding, L. Chen, X. Luo, F. M. He, Y. F. Xiao and Y. Z. Wang, *Chin. Chem. Lett.*, 2022, **33**, 3245–3248.

7 (*a*) Y. Yang, E. M. Terentjev, Y. Wei and Y. Ji, *Nat. Commun.*, 2018, **9**, 1906; (*b*) J. Wu, L. Gao, Z. Guo, H. Zhang, B. Zhang, J. Hu and M. H. Li, *Green Chem.*, 2021, **23**, 5647–5655; (*c*) P. G. Falireas, J. M. Thomassin and A. Debuigne, *Eur. Polym. J.*, 2021, **147**, 110296.

8 (*a*) Y. Yang, S. Zhang, X. Zhang, L. Gao, Y. Wei and Y. Ji, *Nat. Commun.*, 2019, **10**, 3165; (*b*) M. Capelot, M. M. Unterlass, F. Tournilhac and L. Leibler, *ACS Macro Lett.*, 2012, **1**, 789–792.

9 (*a*) X. Feng, J. Fan, A. Li and G. Li, *ACS Appl. Mater. Interfaces*, 2019, **11**, 16075–16086; (*b*) S. Debnath, S. Kaushal and U. Ojha, *ACS Appl. Polym. Mater.*, 2020, **2**, 1006–1013.

10 (*a*) T. Liu, S. Zhang, C. Hao, C. Verdi, W. Liu, H. Liu and J. Zhang, *Macromol. Rapid Commun.*, 2019, **40**, 1800889; (*b*) C. Hao, T. Liu, S. Zhang, W. Liu, Y. Shan and J. Zhang, *Macromolecules*, 2020, **53**, 3110–3118.

11 (*a*) Y. Liu, B. Wang, S. Ma, X. Xu, J. Qiu, Q. Li, S. Wang, N. Lu, J. Ye and J. Zhu, *Eur. Polym. J.*, 2021, **144**, 110236; (*b*) O. Zabihi, M. Ahmadi, R. Yadav, R. Mahmoodi, E. Naderi Kalali, S. Nikafshar, M. R. Ghandehari Ferdowsi, D. Y. Wang and M. Naebe, *ACS Sustainable Chem. Eng.*, 2021, **9**, 4463–4476.

12 (*a*) X. Feng and G. Li, *ACS Appl. Mater. Interfaces*, 2020, **12**, 57486–57496; (*b*) S. Majumdar, H. Zhang, M. Soleimani, R. A. T. M. van Benthem, J. P. A. Heuts and R. P. Sijbesma, *ACS Macro Lett.*, 2020, **9**, 1753–1758.

13 (*a*) H. B. Chen, L. Chen, Y. Zhang, J. J. Zhang and Y. Z. Wang, *Phys. Chem. Chem. Phys.*, 2011, **13**, 11067–11075; (*b*) D. Shen, Y. J. Xu, J. W. Long, X. H. Shi, L. Chen and Y. Z. Wang, *J. Anal. Appl. Pyrolysis*, 2017, **128**, 54–63; (*c*) B. W. Liu, H. B. Zhao and Y. Z. Wang, *Adv. Mater.*, 2022, **34**, 2107905.

14 (*a*) Y. J. Xu, L. Chen, W. H. Rao, M. Qi, D. M. Guo, W. Liao and Y. Z. Wang, *Chem. Eng. J.*, 2018, **347**, 223–232; (*b*) M. M. Velencoso, A. Battig, J. C. Markwart, B. Schartel

and F. R. Wurm, *Angew. Chem., Int. Ed.*, 2018, **57**, 10450–10467.

15 (*a*) J. Gorham, J. Torres, G. Wolfe, A. d'Agostino and D. H. Fairbrother, *J. Phys. Chem. B*, 2005, **109**, 20379–20386; (*b*) A. M. Puziy, O. I. Poddubnaya, R. P. Socha, J. Gurgul and M. Wisniewski, *Carbon*, 2008, **46**, 2113–2123.

16 (*a*) Z. Tang, Y. Liu, B. Guo and L. Zhang, *Macromolecules*, 2017, **50**, 7584–7592; (*b*) Y. Li, T. Liu, S. Zhang, L. Shao, M. Fei, H. Yu and J. Zhang, *Green Chem.*, 2020, **22**, 870–881.

17 (*a*) J. H. Chen, J. H. Lu, X. L. Pu, L. Chen and Y. Z. Wang, *Chemosphere*, 2022, **294**, 133778; (*b*) X. F. Liu, B. W. Liu, X. Luo, D. M. Guo, H. Y. Zhong, L. Chen and Y. Z. Wang, *Chem. Eng. J.*, 2020, **380**, 122471.

18 (*a*) Y. J. Xu, X. H. Shi, J. H. Lu, M. Qi, D. M. Guo, L. Chen and Y. Z. Wang, *Composites, Part B*, 2020, **184**, 107673; (*b*) X. Xu, S. Ma, J. Wu, J. Yang, B. Wang, S. Wang, Q. Li, J. Feng, S. You and J. Zhu, *J. Mater. Chem. A*, 2019, **7**, 15420–15431; (*c*) X. Zhao, X. L. Wang, F. Tian, W. L. An, S. Xu and Y. Z. Wang, *Green Chem.*, 2019, **21**, 2487–2493.

19 B. W. Liu, L. Chen, D. M. Guo, X. F. Liu, Y. F. Lei, X. M. Ding and Y. Z. Wang, *Angew. Chem., Int. Ed.*, 2019, **58**, 9188–9193.

20 (*a*) K. A. Salmeia and S. Gaan, *Polym. Degrad. Stab.*, 2015, **113**, 119–134; (*b*) S. Huo, P. Song, B. Yu, S. Ran, V. S. Chevali, L. Liu, Z. Fang and H. Wang, *Prog. Polym. Sci.*, 2021, **114**, 101366.

21 (*a*) J. H. Chen, W. Q. Yuan, Y. D. Li, Y. X. Weng and J. B. Zeng, *ACS Sustainable Chem. Eng.*, 2019, **7**, 15147–15153; (*b*) F. Lossada, D. Jiao, D. Hoenders and A. Walther, *ACS Nano*, 2021, **15**, 5043–5055.

22 X. Feng, J. Fan, A. Li and G. Li, *ACS Sustainable Chem. Eng.*, 2020, **8**, 874–883.

23 (*a*) X. Feng and G. Li, *Chem. Eng. J.*, 2021, **417**, 129132; (*b*) L. Lu, J. Pan and G. Li, *J. Mater. Chem. A*, 2017, **5**, 21505–21513; (*c*) L. Zhou, G. Zhang, Y. Feng, H. Zhang, J. Li and X. Shi, *J. Mater. Sci.*, 2018, **53**, 7030–7047; (*d*) T. Liu, C. Hao, S. Zhang, X. Yang, L. Wang, J. Han, Y. Li, J. Xin and J. Zhang, *Macromolecules*, 2018, **51**, 5577–5585.